Surface Science 135 (1983) 243–260
North-Holland Publishing Company

SURFACE BEHAVIOUR OF NCO SPECIES ON Rh(111) AND POLYCRYSTALLINE Rh SURFACES

J. KISS and F. SOLYMOSI

Reaction Kinetics Research Group, University of Szeged, P.O. Box 105, H-6701 Szeged, Hungary

Received 3 May 1983; accepted for publication 21 June 1983

The adsorption and surface dissociation of HNCO on Rh surfaces has been investigated by Auger electron, electron energy loss and thermal desorption spectroscopy. Following the adsorption of HNCO on clean Rh(111) and Rh foil at 100 K three adsorbed states can be distinguished by thermal desorption measurements: (i) physisorbed HNCO desorbing at 130 K, (ii) chemisorbed HNCO desorbing at 200 K, and (iii) dissociatively adsorbed HNCO decomposing to various products at higher temperatures. These products are: H_2 (T_p = 280 K), CO (T_p = 450–480 K), N_2 (T_p = 670 and 790 K) and very small amount of NH_3 (T_p = 415 K). No desorption of N_2 was observed from Rh foil up to 900 K. This *was attributed to the boron contamination, which segregated to the surface at higher temperature, and formed a very stable surface species with N.* The adsorption of HNCO at 100 K produced a very intense loss at 10.4 eV and a less intense one at 13.5 eV in the electron energy loss spectra in the electronic range. From the behaviour of these losses at higher temperature it was inferred that the dissociation of adsorbed NCO species to adsorbed N and CO begins to an appreciable extent above 150 K, and that the dissociation is complete at 360–380 K.

1. Introduction

Rhodium is an effective catalyst for the NO + CO reaction; moreover, it is an important constituent of the three-way catalysts used in automobile exhaust catalysis [1–3]. For establishment of the reaction mechanism it is of paramount importance to identify the nature and the role of the surface complex formed during the catalytic reaction. Infrared spectroscopic measurements have revealed that in the NO + CO reaction on supported Rh an isocyanate (NCO) surface complex is formed [4–6]. Further work has disclosed that the support exerts an unexpectedly profound influence on the reactivity of the NCO species [7–11]. In order to evaluate this influence and to determine the surface behaviour of the NCO species on the metal itself (without using any support), we have recently examined the adsorption and surface dissociation of HNCO on Cu(111) [12,13] and Pt(110) [14] surfaces by Auger electron, electron energy loss and thermal desorption spectroscopy. On a clean Cu(111) surface no adsorption of HNCO occurred at 300 K. Preadsorbed oxygen, however, exerted a marked influence and caused the dissociative adsorption of HNCO.

0039-6028/83/0000–0000/$03.00

The NCO species was found to be stable up to about 400 K; when it reacted with chemisorbed oxygen to yield $CO_{2(g)}$ and adsorbed nitrogen atoms, which desorbed as N_2 above 700 K. Above 800 K the formation of C_2N_2 was also detected [13,15].

In contrast, HNCO adsorbed on clean Pt surfaces even at 300 K [14,16]. The NCO species formed, however, was very unstable at this temperature and decomposed further to adsorbed CO and nitrogen atom. EEL spectroscopic measurements in the electronic [14] and in the vibrational range [16], showed that the dissociation of the adsorbed NCO species on Pt(110) begins to an appreciable extent at around 230 K. Recent high-resolution EEL spectroscopic studies on a Pt(110) surface confirmed the high instability of the NCO species on Pt and disclosed further details of the surface processes occurring following HNCO adsorption [17,18]. The most important observation in these studies was the establishment of the high stabilizing effect of preadsorbed oxygen on the NCO species on the Pt(110) surface [17,18].

In the present paper we report on the nature and stability of the NCO species on the Rh(111) surface. In order to have a stronger link with the real catalyst surface, the experiments were extended to polycrystalline Rh foil, too. Another reason for the study of Rh foil is to establish the effect of boron contamination on the behaviour of N-containing compounds on a metal surface.

2. Experimental

The Rh crystal was cut from single crystal rod (Material Research Corporation, 99.999% purity) to within 0.5° and mechanically polished using alumina grain and diamond. The oriented disk-shape crystal was $\sim 6 \times 1$ mm. Rh foil (99.9% purity, 10×10 mm and 0.127 mm thick) was obtained from Hicol Corporation. Both samples were spot-welded between two tungsten wires which themselves were fixed to two Ta foils mounted on a crystal manipulator. They were heated resistively and their temperature was measured with a chromel–alumel thermocouple. For low temperature measurements the Rh samples were cooled through a Ta foil spotwelded to the back-side of the sample and connected to a liquid-nitrogen-cooled stainless steel tube.

The cleaning procedure was the same as used before [19–21]. It consisted of cycles of argon ion bombardment (typically 600 eV, 1×10^{-6} Torr Ar, 300 K, 3 μA for 10–30 min), oxygen treatment and annealing at 1270 K for some minutes. The major contaminants were B, P, S and C. The P, C and S were easily removed, but the removal of B required more extensive cleaning treatments. This was particularly valid for the Rh foil where the B persistently segregated to the surface. In this case a weak signal due to B contamination was always present on the Auger spectra.

HNCO was prepared by the reaction of saturated aqueous KOCN solution with 95% H_3PO_4 at 300 K [13,14]. It was purified by distillation under HV and UHV conditions. It was kept in a glass tube at the temperature of liquid N_2. HNCO vapour was introduced into the chamber (by warming up to 300 K) from an auxiliary vacuum system pumped by a small ion pump through a stainless steel tube with diameter of 0.8 cm. The Rh sample was positioned about 10 mm in front of the effusion hole.

The experiments were carried out in a Varian ion pumped UHV system which was equipped with a single-pass CMA (PHI), with a 3-grid retarding field analyzer (VG) and with a quadrupole mass analyzer. The base pressure was of 1.5×10^{-10} Torr.

For electron energy loss spectra the gun of CMA was used as a primary electron source with energies between 20–125 eV and a beam current of 0.2–1.0 μA [13–15]. The backscattered electrons were analyzed with CMA. A modulation voltage of 0.1 eV was found to be the optimum for the used system. The velocity of taking a spectrum was 0.4 eV/s. The exact position of the peak maxima of energy losses were determined by a Keithley electrometer. Electron energy loss spectra were taken in $dN(E)/dE$ form.

Auger spectra were taken with 3 V peak-to-peak modulation, 1–10 μA of incident current, 2.5 kV of incident energy, and a sweep rate of 3 V/s. In the thermal desorption measurements the sample was in the line-of-sight of MS; about 40 mm to the analyzer.

3. Results

3.1. Adsorption of HNCO at 300 K

3.1.1. AES studies

Exposure of the surface of HNCO at 300 K resulted in the appearance of C, N and O Auger signals at 272, 380 and 508 eV. As was observed in the case of HNCO adsorption on the Pt(110) surface [14], the O Auger signal is very sensitive to the electron beam. There was less effect on the C Auger signal. Determination of the exact value of the C Auger signal, however, was difficult, as this signal appeared very near one of the main Rh Auger signals (258 eV). The intensity of the N Auger signal was not influenced by the electron beam; and this was used to determine the saturation coverage attained at 10 L (fig. 1).

The initial sticking probability was estimated graphically from plots of the relative N Auger signal versus HNCO exposure (fig. 1). A value of 0.6 was found, which is larger than that calculated for the Pt(110) surface [14].

In order to facilitate the interpretation of the TPD spectra, the sample saturated with HNCO was heated to different temperatures and the changes in the N and C Auger signals were monitored at 300 K. The results are also

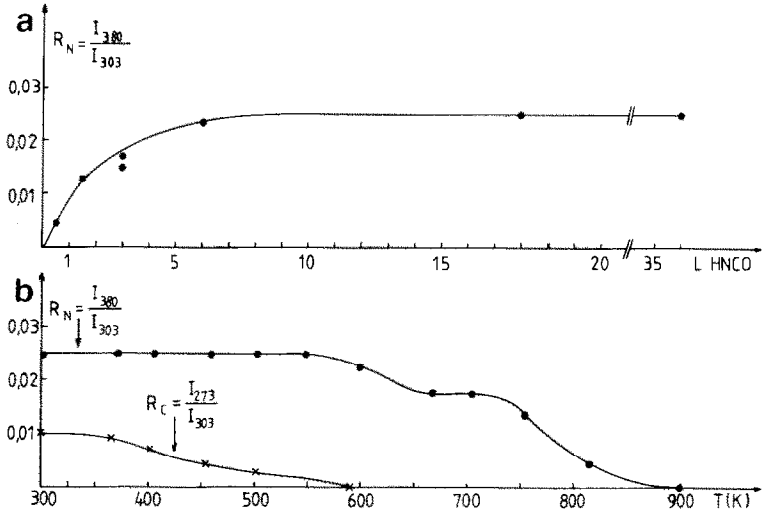

Fig. 1. The dependence of the relative N signal on the HNCO exposure on Rh(111) at 300 K (a) and that of the relative N and C signals on the temperatures (b).

shown in fig. 1. The intensity of the C Auger signal was attenuated slightly above 350 K, and it was hardly detectable above 580 K. In contrast, the N Auger signal did not change up to 550 K, and it began to decrease only above this temperature, in two stages: 550–660 K and 720–900 K.

3.1.2. Thermal desorption studies

After saturation of HNCO on the Rh(111) surface at 300 K, desorption of NH_3, N_2 and CO was recorded (fig. 2). There was no indication of the desorption of HNCO. A small amount of H_2 was also detected. It should be mentioned that H_2 evolution was observed even during the adsorption of HNCO, its extent being larger than that resulting from the fragmentation of HNCO in the mass spectrometer. The peak maximum of NH_3 desorption appeared at 415 K. The largest desorption, three well-separated peaks (T_p = 450–480, 670 and 790 K), was given by 28 amu (N_2, CO). Differentiation between N_2 and Co was made via careful analysis of the intensity ratios of the signals at 12 amu (CO), 14 amu (N) and 28 amu (CO and N_2). The signal at 12 amu produced one peak at 450–480 K; this corresponds to the low-temperature peak of the 28 amu signal. With the rise of HNCO exposure, a shoulder appeared on the low-temperature side of the peak above 2 L HNCO. The signal at 14 amu yielded the other two peaks, T_p = 670 and 790 K. These peak temperatures showed no variation with the increase of the coverage. The TPD results for the desorption of CO and N_2 are in good agreement with the Auger data presented in fig. 1. (The desorption of a small amount of NH_3 caused

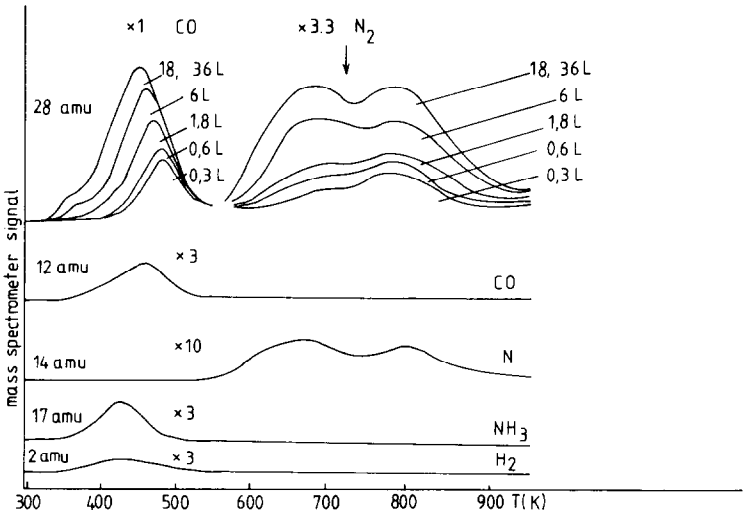

Fig. 2. Thermal desorption spectra following HNCO adsorption at 300 K on Rh(111) surface. The curves are uncorrected for detection sensitivities.

only slight change in the intensity of the N Auger signal.) With the assumption of a "normal" pre-exponential for desorption (10^{13} s^{-1} for first-order desorption), the following desorption energies were calculated from the peak temperatures: 120.5 kJ/mol for CO, and 168 and 198 kJ/mol, respectively, for N_2.

The surface coverage was calculated by comparing the amount of CO desorbed from the surface saturated by HNCO at 300 K with the value obtained after CO adsorption alone [22].

In this way we established that, following the adsorption and surface decomposition of HNCO on Rh(111), there are 5×10^{14} molecules CO per cm^2 on the surface. We calculated practically the same value by accurate determination and comparison of the C Auger signals obtained after HNCO and CO adsorption to saturation.

Neglecting the small amount of NH_3 formed on the surface (which is less than 3% of the nitrogen desorbed), on the basis of the equation

$$NCO_{(a)} \rightarrow N_{(a)} + CO_{(a)}, \quad (1)$$

we can assume that the same amount of adsorbed N atoms exists on the surface.

3.1.3. Electron energy loss studies

In the examination of the dependence of the elastic peak height reflected from a clean Rh foil on the primary energy, a maximum reflectance was found slightly above 70 eV. The characteristic loss energies of the Rh foil occurred at

5.0, 19.6 and 24.5 eV; these losses showed little variation with the primary electron energy. It should be noted that on a carefully cleaned Rh surface (bombardment with argon ions and subsequent heat treatment at 1200 K), we did not observe the losses at 7.9 and 8.7 eV found by previous authors with other techniques (see section 4.1.2).

Exposure of the Rh surface to HNCO resulted in an increase of the elastically back-scattered electrons (i.e. the elastic peak) by a factor of 1.35. A similar increase was observed in the loss at 5.0 eV. In contrast, the adsorption of HNCO reduced the intensities of the losses at 19.6 and 24.5 eV. A new loss appeared only at 13.5 eV, its intensity increasing up to 10 L HNCO exposure. Under special conditions–registration of the EEL spectrum immediately (< 2 min) after HNCO adsorption and only in the limited energy range – a weak loss was also detected at 10.4 eV. This loss feature, however, completely disappeared after 3–5 min.

The loss at 13.5 eV was much more stable; it decreased only when the sample was warmed up to 388 K, and was eliminated only at around 510 K.

3.2. Adsorption of HNCO at 95 K

3.2.1. Thermal desorption studies

As indicated by the AES signals, the extent of HNCO adsorption is greatly increased at this temperature. Adsorption is very rapid, indicating an initial sticking probability close to unity.

In this case the desorption of HNCO (43 amu) was also observed; it started simultaneously with the onset of the temperature program. An initial peak

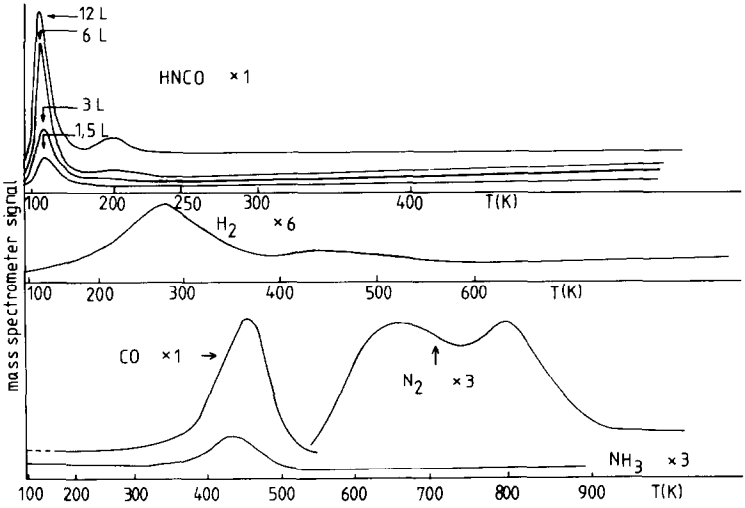

Fig. 3. Thermal desorption spectra following HNCO adsorption at 95 K on Rh(111) surface. The curves are uncorrected for detection sensitivities.

occurred at 130 K and grew with exposure. A much smaller peak was registered at 200 K above 6 L (fig. 3). In this case a larger amount of hydrogen desorbed with peak temperature $T_p = 280$ K, and a very small amount at 420 K. NH_3 is again desorbed in a single pulse, with peak temperature $T_p = 420$ K. The desorption of CO and N_2 was observed only at high temperatures, with practically the same peak temperatures as after adsorption at 300 K. The amounts of desorbed CO and N_2 agreed quite well with those obtained following HNCO adsorption at 300 K.

A quantitative analysis of the respective peak areas, taking into account the individual differences in mass spectrometer sensitivity and pumping rate for various species, reveals that approximately $\sim 4 \times 10^{15}$ molecules HNCO per cm^2 desorb at 100–230 K. The concentration of irreversibly adsorbed HNCO, which is transformed and decomposed into NH_3, H_2, N_2 and CO, is $\sim 5 \times 10^{14}$ molecules per cm^2, whereas $\sim 5 \times 10^{14}$ molecules CO and $\sim 2.4 \times 10^{14}$ N_2 molecules per cm^2 are desorbed at higher temperatures.

3.2.2. Electron energy loss studies

The EEL spectrum of the Rh(111) surface after cleaning showed a weak loss at 13.2–13.5 eV, indicating that a small amount of CO from the background was adsorbed on the Rh during cooling (fig. 4). Exposure of the Rh(111) surface to HNCO at 95 K produced an intense loss at 10.4 eV and at the same time enhanced the intensity of the loss at 13.5 eV (fig. 4). A decrease in the intensities of the 19.6 and 24.5 eV losses was observed in this case, too.

EEL spectra obtained after heating of the HNCO-saturated sample from 95 K to different temperatures are also shown in fig. 4. The intensity of the loss at 10.4 eV decreased gradually and was eliminated above 343 K. In contrast, the intensity of the 13.5 eV loss decreased only from 95 to 140 K; it afterwards increased considerably up to about 390 K but then progressively decreased.

It should be kept in mind that, in these experiments, after heating of the Rh crystal to a selected temperature, and recording of the spectra at 95–100 K, the sample was cleaned and then exposed again to fresh HNCO. This means that the intensities of the losses obtained are not affected by the beam and thermal effect of previous measurements. The sample was cooled immediately (2–5 s) after reaching the selected temperature. This was probably the reason that in this case the 10.4 eV loss was identified even after warming up the sample to 343 K.

3.3. HNCO adsorption on Rh foil

The above experiments were repeated on Rh foil. Only the main results are summarized here. Based on the changes in the N Auger signal, at 95 K saturation coverage was reached at ~ 16 L. This value was 12 L at 300 K. Following HNCO adsorption at 95 K, desorption of HNCO, H_2, NH_3, CO

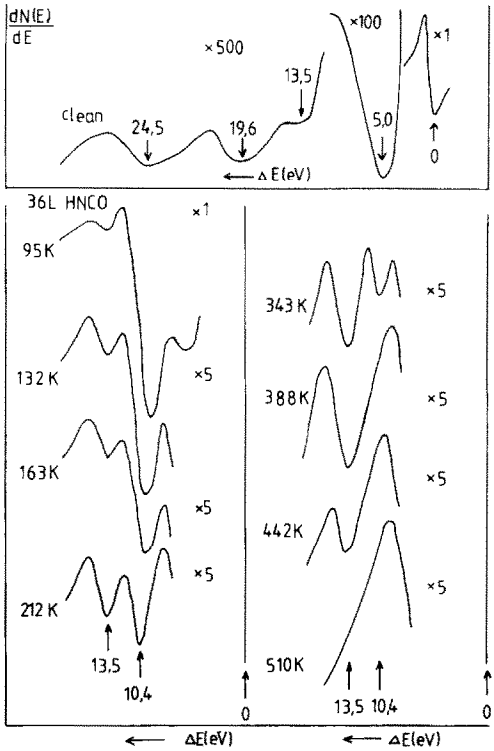

Fig. 4. (a) Electron energy loss spectrum of clean Rh(111) at 95 K. (b) Electron energy loss spectra taken after heating the Rh(111) surface to different temperatures. The surface was exposed to 36 L HNCO at 95 K before heating.

and N_2 was observed (fig. 5). When the adsorption of HNCO was performed at 300 K, no HNCO or NCO-containing compounds were detected in the desorbing gases (fig. 5).

Although these data will be compared in the discussion, section 4, with those obtained on the Rh(111) surface, it must be pointed out here that, in contrast to the Rh(111) surface, no desorption of nitrogen was observed from this surface at 550–900 K. A very limited (if any) nitrogen desorption occurred at around 950 K. The situation was the same when the HNCO was admitted onto the Rh foil sample before or after thermal treatment at 1240 K, following Ar ion bombardment. This behaviour was confirmed by Auger spectroscopic measurements, which showed only an extremely slight decrease in the intensity of the N Auger signal (less than 1%) up to 1240 K.

The EEL spectrum of clean Rh foil agreed well with that of the Rh(111) surface (fig. 6). There was no significant difference when the clean sample was heated to 1000 K to promote the segregation of boron from the bulk to the surface.

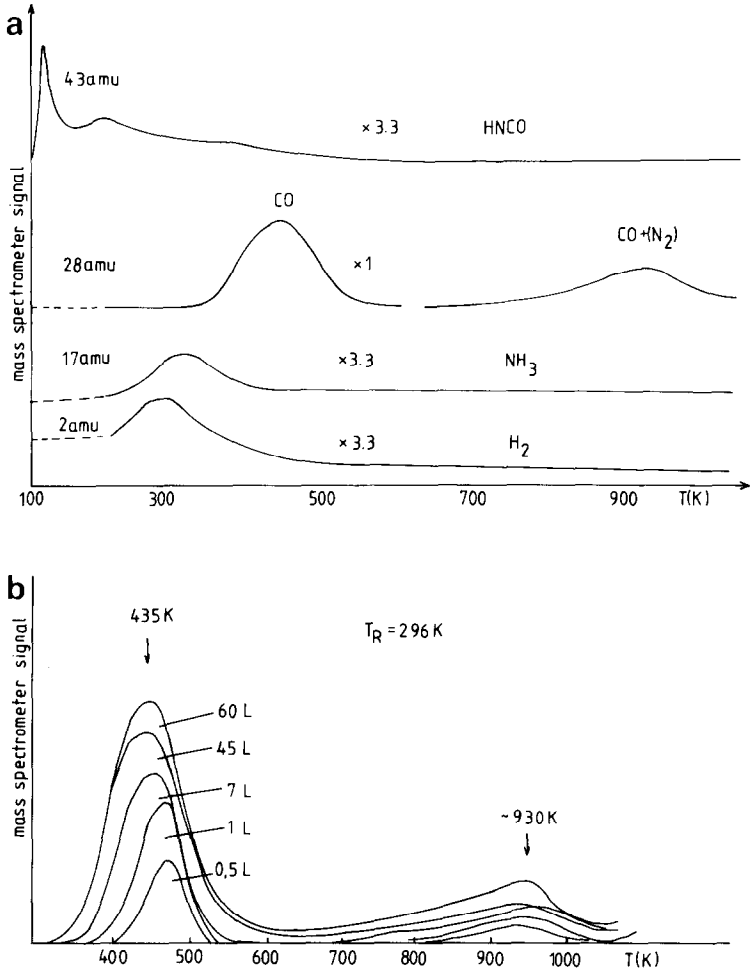

Fig. 5. (a) Thermal desorption spectra following HNCO adsorption on Rh foil. (b) Thermal desorption spectra for 28 amu following HNCO adsorption on Rh foil. The curves are uncorrected for detection sensitivities.

Adsorption of HNCO at 95 K produced a very intense loss at 10.4 eV, its intensity increasing with the HNCO exposure (fig. 6). A significant enhancement of the loss at 13.5 eV, already observed on the "clean" surface, again occurred; its intensity, however, was less than that of the 10.5 eV loss.

When the Rh sample containing multilayer HNCO was heated up to different temperatures, in the same manner as in the case of the Rh(111) surface, the intensity of the 10.5 eV loss gradually decreased up to 296 K, when it was eliminated. The loss at 13.5 eV was also attenuated with the rise of the

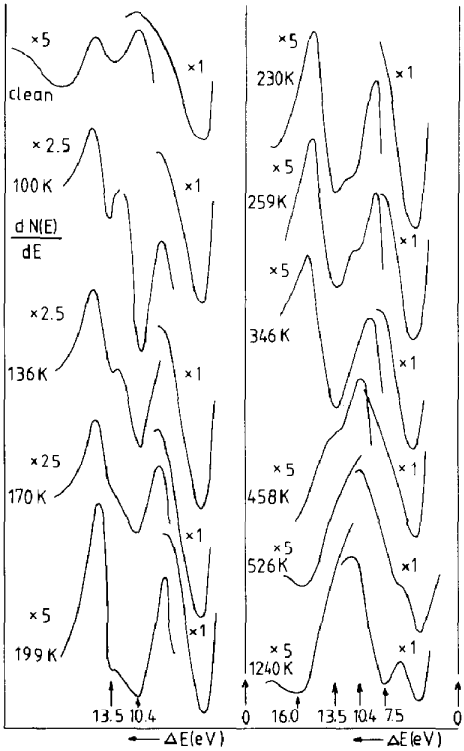

Fig. 6. Electron energy loss spectra taken after heating the Rh foil to different temperatures. The surface was exposed to 90 L HNCO at 100 K before heating.

temperature up to 177 K, but afterwards it slightly increased. It began to decrease only above 300 K, and disappeared at 526 K.

Above 520 K, strong losses appeared at 7.3–7.5 and 16 eV, the intensities of these losses increased with the rise of the sample temperature, and they did not decrease even at 1240 K. They could be eliminated only by Ar ion bombardment.

Adsorption of HNCO at 300 K produced only an intense loss at 13.5 eV, which behaved similarly as that observed for the 300 K adsorption on Rh(111). New losses appeared again, at 7.5–7.8 eV and at 16 eV above 520 K.

4. Discussion

4.1. Rh(111) surface

4.1.1. General characteristics of the surface reaction

The adsorption and surface behaviour of HNCO on Rh(111) is very similar

to that observed on the Pt(110) and Pt(111) surfaces [14,16–18]. The adsorption of HNCO at 95 K, and at high exposures, leads to a multilayer. HNCO was detected in the desorbing gases only after its low-temperature (~ 95 K) adsorption. Desorption occurred in two stages, with peak maxima at 130 and 200 K; the corresponding activation energies are 32 and 50 kJ/mol. A considerable amount of hydrogen is also formed, suggesting that the dissociation of adsorbed HNCO took place in the adsorbed layer. Accordingly, we may count on the following reactions:

$$HNCO_{(g)} \rightleftharpoons HNCO_{(a)}, \tag{2}$$

$$HNCO_{(a)} \rightleftharpoons H_{(a)} + NCO_{(a)}, \tag{3}$$

$$HNCO_{(a)} \rightleftharpoons HNCO_{(g)}, \tag{4}$$

$$H_{(a)} + H_{(a)} \rightleftharpoons H_{2(g)}, \tag{5}$$

$$H_{(a)} + NCO_{(a)} \rightleftharpoons HNCO_{(a)} \rightleftharpoons HNCO_{(g)}. \tag{6}$$

We assume that the desorption of chemisorbed HNCO (step (4)) is responsible for the desorption peak at 200 K, but the occurrence of reaction (6) also contributes to the development of this desorption stage. The irreversibly adsorbed HNCO occupies only 30% of the Rh(111) surface provided that HNCO (or more probably NCO) is bonded to one Rh atom. Hydrogen desorbed in one stage: $T_p = 280$ K. This temperature value is somewhat lower than that found following H_2 adsorption on the Rh(111) surface [23].

Above 380 K the desorption of a small amount of NH_3 ($T_p = 415$ K) was also observed. Note that no NH_3 desorption was observed following NH_3 adsorption on Rh(110) surface at 250 K, however, the rates of NH_3 decomposition on this surface were over 10 times as great as those on the Rh(111) surface [26]. Although the slight contamination of HNCO with NH_3 cannot be excluded, this NH_3 being formed in the hydrolysis of HNCO in the presence of H_2O in the system, we believe that this source of NH_3 is negligible. It is more probable that NH_3 is formed in the surface reaction of NCO species. This may occur in a direct reaction between adsorbed NCO and activated hydrogen, as was observed in the case of supported metal [4–11]:

$$NCO_{(a)} + 3\ H_{(a)} \rightleftharpoons NH_{3(a)} + CO_{(a)}, \tag{7}$$

or the nitrogen atom formed in the dissociation of NCO,

$$NCO_{(a)} \rightarrow N_{(a)} + CO_{(a)}, \tag{8}$$

reacts with hydrogen.

An alternative route for the formation of NH_3 is that in the adsorbed HNCO the HN–CO bond breaks and $NH_{(a)}$ and $CO_{(a)}$ are formed:

$$HNCO_{(a)} \rightleftharpoons HN_{(a)} + CO_{(a)}. \tag{9}$$

The $NH_{(a)}$ species can be hydrogenated further or undergo disproportionation and desorbs in the form of NH_3. This route is supported by the thermodynamic data [24], as in the case of gaseous HNCO, the N–H bond is weaker than the N–C bond; D(H–NCO) = 4.90 eV, D(HN–CO) = 3.38 eV, D(HNC–O) = 2.14 eV. Accordingly, in the photolysis of HNCO a significant amount of HN radical was found [24,25].

The nature of the adsorbents and the bonding mode of the molecule may alter the picture basically, however, and taking into account the results relating to HNCO adsorption, there is no evidence yet that reaction (9) occurs on solid surfaces.

The formation of NH_3 was observed following HNCO adsorption on the Pt(110) and (111) surfaces [14,16,18]. The adsorption of HNCO on the Pt(110) surface at 155–200 K produced a very strong band at 3385 cm^{-1} on the HREEL spectra [18]. As there was no sign of the 2260 cm^{-1} band, ν_{as}(NCO), characteristic of the gaseous and weakly adsorbed HNCO molecule, the appearance of the 3350 cm^{-1} band may indicate that the formation of NH_x species occurs in the adsorbed layer at 155–200 K. This band was strong and it was present even up to 350 K, where NCO decomposed completely.

When the sample temperature was raised, first CO, and then from 550 K N_2 evolution was observed. The desorption temperature of CO agreed well with that reported following CO adsorption on Rh(111) surfaces at such coverage [22,27]. It is interesting that the nitrogen desorbed at significantly higher temperatures, T_p = 670 and 790 K, than from the Pt(110) surface [28]. The low-temperature desorption peak correlates quite well with the N_2 peaks obtained following adsorption of NO on Rh wire [29] and that of NH_3 on Rh crystals [26]. In order to know more about the Rh + N interaction, in separate work we investigated the adsorption of N atoms on the Rh(111) surface [30]. We found that at high coverage ($\theta \approx 0.5$) the main desorption peak of nitrogen was at 416 K. At low coverage corresponding to that found after HNCO adsorption, however, the desorption was observed only above 600 K, with peak temperatures T_p = 663 and 790 K. We assume that the latter peak is caused by small amounts of impurity boron that segregate to the Rh surface above 700 K.

These results indicate that *the formation of the two species is a process limited not by the reaction, but rather by the desorption rate.* Thus, the dissociation of adsorbed NCO (step (8)) proceeds at or (more likely) below the desorption temperature of CO.

When the adsorption of HNCO was performed at 300 K, the basic difference was that we could no detect the desorption of HNCO. The amount of H_2 desorbed was also less, as the low-temperature peak (T_p = 280 K) was missing, and H_2 formed even during the adsorption of HNCO. The desorption characteristics of other gases were the same as following HNCO adsorption at 95 K.

4.1.2. Electron energy loss measurements

Before discussing the EEL spectra caused by HNCO, we have to deal briefly with *the characteristic energy losses of the clean Rh surface.*

Lynch and Swan [31] first investigated the EEL spectrum of Rh; this exhibited a strong peak at 7.9 eV with a full-width at half-maximum of approximately 3 eV, and a somewhat broader peak at 24.6 eV. The authors suggested that the 7.9 eV loss is due to the excitation of a surface plasmon and the 24.6 eV peak to a volume plasmon. Staib and Ulmer [32] measured the EEL spectra of Rh foil under $(1-5)\times 10^{-8}$ Torr at the primary energy of 200–800 eV with a total scattering angle of 45°. They used an electrostatic electron analyzer. Peaks were found at 8.6, (16), 26 and 35 eV.

The characteristic losses of Rh were also calculated from optical measurements [33–37]. In most cases the Rh films were prepared by electron gun evaporation. Losses were found at 7.9–8.1 [33,34], 8.7–9 [33,34,36,37] and 32.5–33 eV [33–36].

In our measurements on carefully cleaned Rh surfaces, we observed losses at 4.1–5.4, 19.6 and 24.5 eV. The positions of these losses remained unaltered at primary energies of 40–100 eV. The basic difference between the loss spectra obtained in this work and previous ones is that we have not detected any loss features at 8.7–9.0 and 7.9–8.1 eV.

Great care is to be exercised in the comparison of loss features determined by different methods. It should be taken into account that even the same method, e.g. the determination by electron energy analyzer of characteristic energy losses of low-energy electrons, back-scattered from metal surfaces, can yield somewhat different loss values from the same data, if the EEL spectrum is taken in $\mathrm{d}N/(E)/\mathrm{d}E$ or $N(E)$ form.

In $\mathrm{d}N(E)/\mathrm{d}E$ spectra, loss values are given as distances between the minima of $\mathrm{d}N/\mathrm{d}E$ for the elastic peak and the loss features, i.e. the distances of the high-energy inflection points of the $N(E)$ curves, while from $N(E)$ curves the distances of the maxima are taken. The failure to observe losses at 8.7 and 7.9 eV in the present work, however, cannot be accounted for by the fact that we have taken the EEL spectrum in $\mathrm{d}N(E)/\mathrm{d}E$ form. It seems more likely that the different results are due to different degrees of cleanness of the Rh samples. We should emphasize that the present measurements were performed under UHV conditions, where the background pressure was less than 5×10^{-10} Torr. The cleanness of the Rh was checked before every measurement by Auger spectroscopy.

In contrast to this, in the majority of the previous measurements mentioned above, (i) the vacuum conditions were much poorer than in this work, (ii) the sample was only cleaned by thermal treatment, which in our experience is not sufficient to remove all the surface contaminants, (iii) in no other work, even in that carried out under UHV conditions [36], was the sample cleanness checked by Auger spectroscopy.

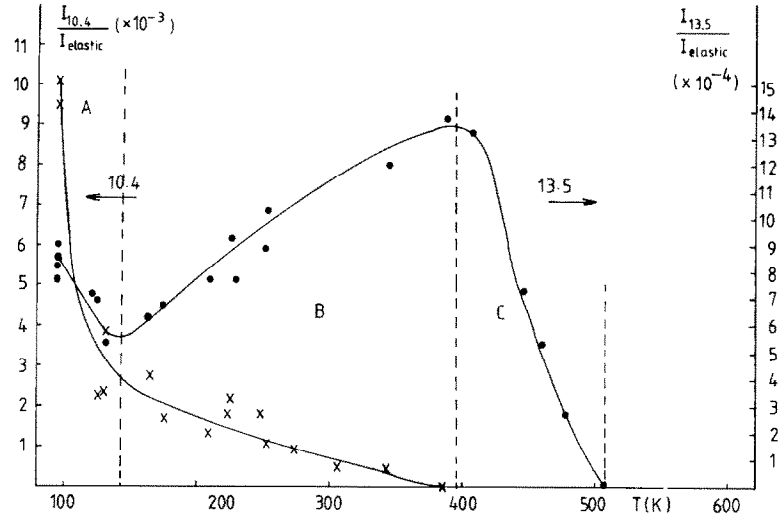

Fig. 7. The intensities of (×) 10.4 and (●) 13.5 eV losses related to the elastic peak after heating the Rh(111) surface to different temperatures. The surface was exposed to 36 L HNCO at 95 K before heating.

Accordingly, we are inclined to think that in the previous studies the Rh samples were not sufficiently clean and the losses observed at 8.7–9 and at 7.9–8.1 eV might have been caused by surface contaminants.

One of the possible candidates for this is boron. The presence of boron on the surface, as was shown in ref. [21], does not give any new losses but it forms a very stable surface species with oxygen [21] and nitrogen [30] which produce intense losses at 9.3 and 7.7 eV, respectively (see later).

The adsorption of HNCO on the Rh(111) surface at 100 K produced new losses at 10.4 and 13.5 eV. When the adsorption was performed at 300 K, these losses were observed only when the EEL spectra were taken immediately (< 2 min) after HNCO adsorption. We attribute both losses to adsorbed isocyanate compounds. This assumption is based on the results obtained on the Cu(111) surface. The adsorption of HNCO on Cu(111) (predosed with oxygen) at 300 K resulted in intense losses at 10.4 and 13.5 eV [13]. As neither CO, nor CO_2, adsorbs on a clean and oxygen-dosed Cu surface at 300 K, we could exclude the contribution of these species to the loss feature observed following HNCO adsorption. It may be noted that none of the other decomposition or reaction products (N, H, NH_3) gave losses in this energy range. Furthermore, these losses were also observed when the NCO species was produced on the Pt(110) surface at 100 K [14], and thus the EEL spectrum of adsorbed NCO is now well documented. As regards the assignment of these losses, however, further work and speculation are needed.

As concerns the events occurring on the adsorbed layer at elevated temperatures, the examination of EEL spectra is the most promising. For this purpose we plotted the intensities of the losses in fig. 7 as a function of the temperature to which the sample was heated. The intensity of the loss at 10.4 eV decreased sharply up to 140 K, and more slowly up to 360–380 K, where it was eliminated. In contrast, the intensity of the 13.5 eV loss decreased only up to about 140–150 K, somewhat more slowly than that of the 10.4 eV loss; afterwards it increased considerably up to about 400 K, and then decreased until complete elimination at 510 K.

As the CO adsorbed on Rh also gives a loss at 13.5 eV [21], the complex behaviour of the 13.5 eV loss corresponds to the desorption of HNCO, the decomposition of NCO and the formation and desorption of adsorbed CO. Taking into account the HNCO desorption peak ($T_p \sim 130$ K), we may conclude that the decrease in the intensities of the 10.4 and 13.5 eV losses up to about 140 K corresponds to the desorption of physisorbed HNCO (we denote this as stage A).

Stage B (140–390 K), when the intensities of the 10.4 and 13.5 eV losses change in the opposite direction, reflects the desorption of chemisorbed HNCO (step (6)) and the decomposition of the NCO species to adsorbed N and CO (step (8)). The fact that the intensity of the 13.5 eV loss increases in this temperature range can be interpreted in such a way that the chemisorbed CO produces a more intense loss than chemisorbed NCO, and that thus the formation of $CO_{(a)}$ overcompensates the diminishing effect of the decomposition of NCO on the intensity of the 13.5 eV loss.

In stage C (390–510 K), the observed decrease in the intensity of the 13.5 eV loss is the result of the desorption of adsorbed CO,

$$CO_{(a)} \rightleftharpoons CO_{(g)}, \tag{10}$$

formed in the surface dissociation of NCO. This is in harmony with the characteristics of the desorption of CO.

4.2. Rh foil

Results similar in many respects were obtained on Rh foil. Saturation occurred at somewhat higher exposures and the sticking coefficient was also higher.

The slight variation observed in the desorption temperatures of the products has probably no relevance to the difference of the interaction of HNCO with Rh foil, and only reflects the differences on the surfaces of the two samples. From a comparison of the EEL spectra of HNCO adsorbed on the two surfaces, it appears that the 10.4 eV loss vanishes at lower temperature on Rh foil than on the Rh(111) surface: accordingly, the NCO species is slightly less stable on Rh foil, which can be accounted for by the higher number of irregularities (steps, kinks and defects) as compared to the Rh(111) surface.

The striking difference between the two surfaces is that while the N_2 starts to desorb from the Rh(111) surface at 580 K, $T_p = 670$ and 790 K, only an extremely limited desorption of N_2 was observed from this surface at around 930 K.

A possible reason for this difference may be sought in the different purities of the Rh samples. While the purity of the Rh(111) is 99.999%, that of the Rh foil is 99.9%. The main contaminant of the Rh foil is boron. As the results presented in fig. 8 show, the surface concentration of boron is remarkably constant up to 700 K, but above this temperature the boron diffuses out from the bulk to the surface. At 1100 K its relative Auger signal is more than five times that measured at 300–700 K. It is very likely that the boron contamination basically alters the adsorptive and bonding properties of the surface. In the present case this is mainly exhibited in the desorption of nitrogen.

Nitrogen forms a very stable species with boron (the dissociation energy of B–N is 389 kJ/mol), which scarcely releases nitrogen below 1200 K. This surface species can be destroyed only by Ar ion bombardment. A similar observation was recently made by Vavere and Hansen [26] in the study of the decomposition of NH_3 on different Rh surfaces.

Hence, the new losses at 7.5–7.8 and 16 eV, observed when the sample was heated to above 500 K, might perhaps be attributed to the formation of boron nitride.

We can exclude the possibility that this loss is merely the result of the presence of surface boron, as no such losses appeared on Rh foil (without HNCO adsorption), even after high-temperature treatment, which causes the segregation of boron on the surface. As the surface concentration of boron did

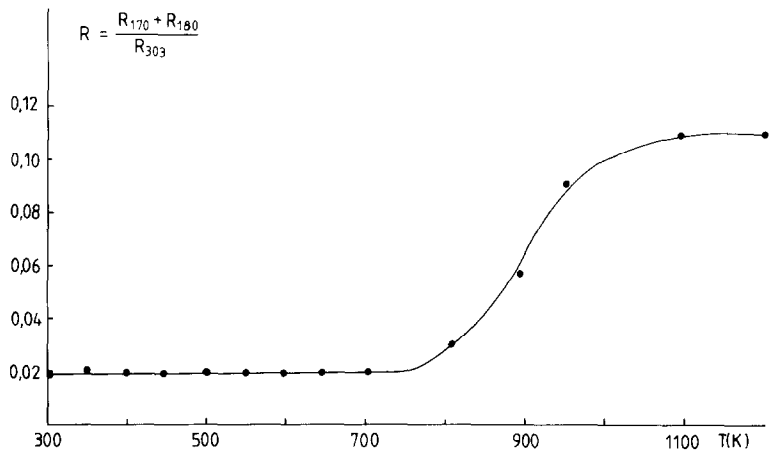

Fig. 8. The dependence of the relative B signal of Rh foil on the temperatures. Auger beam energy 2.5 kV, beam current 10 μA.

not change at 300–700 K (fig. 8), the appearance of these losses by 520 K probably indicates that the nitrogen reacts with boron, or at least that the reaction becomes more significant (detectable) around this temperature.

Further support for this explanation comes from the study of the adsorption of the nitrogen atom on this Rh foil [30]. An intense loss at 7.5–7.8 eV was found following the thermal treatment of the sample exposed to N atoms at 536 K, which exhibited the same behaviour as that observed in this study.

Although the presence of boron drastically changed the bonding of nitrogen to the Rh surface, we have no reason to assume that it influenced the stability of the NCO species, which – we believe – decomposes at much lower temperatures, i.e. before boron interacts with the nitrogen. it is possible, however, that boron contaminants can alter the stability of those N-containing compounds which should desorb from the clean Rh (or other metal) surface at much higher temperatures. Experiments to check this idea are in progress in our laboratory.

5. Conclusions

HNCO adsorbs molecularly on Rh(111) and Rh foil at 95 K, but dissociates at higher temperatures. The NCO formed in the dissociation is an unstable species on Rh surfaces. It starts decomposing around 150 K producing adsorbed N and CO, which desorb only at higher temperatures. According to electron energy loss spectroscopic measurements, NCO decomposes completely on Rh(111) below 390 K. Similar behaviour was experienced on Rh foil. It was observed that the boron contamination of Rh foil greatly influences the desorption of nitrogen by the formation of a stable boron nitride surface compound, which may affect its catalytic activity in the NO–CO reaction.

References

[1] M. Shelef and J.T. Kummer, Chem. Eng. Progr. Symp. Ser. 67 (1971) 74.
[2] K.C. Taylor and J.C. Schlatter, J. Catalysis 63 (1980) 53.
[3] L.L. Hegedüs, J.C. Summers, J.C. Schlatter and K. Baron, J. Catalysis 56 (1979) 321.
[4] M.L. Unland, J. Catalysis 31 (1973) 459.
[5] H. Arai and H. Tominaga, J. Catalysis 43 (1976) 131.
[6] F. Solymosi and J. Sárkány, Appl. Surface Sci. 3 (1979) 68.
[7] F. Solymosi, J. Kiss and J. Sárkány, in: Proc. 7th Intern. Vacuum Congr. and 3rd Intern. Conf. on Solid Surfaces, Vienna, 1977, Eds. R. Dobrozemsky et al., p. 819.
[8] F. Solymosi, L. Völgyesi and J. Sárkány, J. Catalysis 54 (1978) 336.
[9] F. Solymosi, L. Völgyesi and J. Raskó, Z. Physik. Chem. (NF) 120 (1980) 79.
[10] F. Lorimer and A.T. Bell, J. Catalysis 59 (1979) 223.
[11] J. Raskó and F. Solymosi, JCS Faraday Trans. I, 76 (1980) 2383.
[12] F. Solymosi and J. Kiss, in: Proc. IVC-8, ICSS-4 and ECOSS-3, Cannes, 1980, p. 213.

[13] F. Solymosi and J. Kiss, Surface Sci. 104 (1981) 181.
[14] F. Solymosi and J. Kiss, Surface Sci. 108 (1981) 641.
[15] F. Solymosi and J. Kiss, Surface Sci. 108 (1981) 368.
[16] R.J. Gorte, L.D. Schmidt and B.A. Sexton, J. Catalysis 67 (1981) 387.
[17] M. Surman, F. Solymosi, P. Hofmann and D.A. King, J. Catalysis, in press.
[18] M. Surman, F. Solymosi, P. Hofmann and D.A. King, to be published.
[19] B.A. Sexton and G.A. Somorjai, J. Catalysis 46 (1977) 167.
[20] R. Marbow and R.M. Lambert, Surface Sci. 67 (1977) 489.
[21] F. Solymosi and J. Kiss, J. Catalysis 81 (1983) 95.
[22] D.G. Castner, B.A. Sexton and G.A. Somorjai, Surface Sci. 71 (1978) 519.
[23] J.T. Yates, P.A. Thiel and W.H. Weinberg, Surface Sci. 84 (1979) 427.
[24] H. Okabe, J. Chem. Phys. 53 (1970) 3507.
[25] D.E. Milligan and M.E. Jacox, J. Chem. Phys. 47 (1967) 5157.
[26] A. Vavere and R.S. Hansen, J. Catalysis 69 (1981) 158.
[27] P.A. Thiel, A.D. Williams, J.T. Yates and W.H. Weinberg, Surface Sci. 84 (1979) 54.
[28] J. Kiss, A. Berkó and F. Solymosi, in: Proc. IVC-8, ICSS-4 and ECOSS-3, Cannes, 1980, Vol. I, p. 521.
[29] C.T. Campbell and J.M. White, Appl. Surface Sci. 1 (1978) 347.
[30] A. Berkó and F. Solymosi, to be published.
[31] M.J. Lynch and J.B. Swan, Australian J. Phys. 21 (1968) 811.
[32] Ph. Staib and K. Ulmer, Z. Physik 219 (1969) 381.
[33] J.T. Cox, G. Hass and W.R. Hunter, J. Opt. Soc. Am. 61 (1971) 360.
[34] S. Seignac and S. Robin, Compt. Rend. (Paris) B271 (1970) 919.
[35] J.H. Weaver, Phys. Rev. B11 (1975) 1416.
[36] D.T. Pierce and W.E. Spicer, Phys. Status Solidi (b) 60 (1973) 689.